TNO-*report*
TPD-HAG-RPT-960132

Surface excitation: A theoretical and experimental study of strip mobility on a line-stiffened plate

TNO Institute of Applied Physics

Stieltjesweg 1
P.O. Box 155
2600 AD Delft
The Netherlands

Phone (+31) 15 69 20 00
Fax (+31) 15 69 21 11

Date

23 September 1996

Author(s)

Dr.ir. C.A.F. de Jong
Ir. P.P. Kooyman
Ing. F.G.P. van der Knaap

Classification

Classified by	: Ing. H. Hasenpflug
Classification date	: September 1996
	(After 10 years this classification is no longer valid)
Title	: Ongerubriceerd
Executive summary	: Ongerubriceerd
Abstract	: Ongerubriceerd
Report text	: Ongerubriceerd
Appendices A-B	: Ongerubriceerd

Copy no.	: 20
No. of copies	: 20
No. of pages	: 32
	(including appendices, excluding distribution list)
No. of appendices	:

TNO Institute of Applied Physics (TPD) is a contract research organization for industry and government with a multi-disciplinary approach. In-house disciplines are: applied physics, information technology, mechanics, electronics, materials and process technology.

Netherlands organization for applied scientific research

MANAGEMENTUITTREKSEL

Title : Surface excitation: A theoretical and experimental study of strip mobility on a line-stiffened plate

Author(s) : dr.ir. C.A.F. de Jong, ir. P.P. Kooyman & ing. F.G.P. van der Knaap

Date : 23 September 1996

Projectno. : A94/KM/155

IWP-no. : 797

TPD projectno. : 627.190

Reportno. : TPD-HAG-RPT-960132

Aanleiding tot het onderzoek
In Werkgebied I van het TNO DO-onderzoeksprogramma worden rekenmodellen ontwikkeld voor constructiegeluidoverdracht van machines naar onderwater. Een van de aspecten die daarbij onderzocht worden is het effect van de afmetingen van de contactvlakken tussen machine, fundatie en scheepsbodem op de geluidoverdracht. In een theoretische studie naar lijnaanstoting op balk-achtige constructies, beschreven in TPD-HAG-RPT-930216, is aangetoond dat de geluidoverdracht ten gevolge van stripaanstoting duidelijk afwijkt van die ten gevolge van puntaanstoting, wanneer de lengte van de strip groter of gelijk is aan de helft van de golflengte in de balken. Vanwege het praktische belang voor scheepsconstructies is het onderzoek voortgezet met een studie naar de aanstoting van verstijfde plaat-constructies via grote contactvlakken.

Doel van het onderzoek
Het modelleren van aanstoting van een plaat met een lijnvormige verstijver via grote contactvlakken. Experimenteel valideren van de gevonden modellen.

Werkplan
De verdeelde aanstoting zal worden gemodelleerd door het contactvlak te verdelen in een discreet aantal punten. De totale energieoverdracht wordt vervolgens bepaald door de ingangs- en overdrachtsadmittanties en de krachtverdeling voor deze punten in rekening te brengen. De resultaten van modelberekeningen zullen worden gevalideerd aan de hand van laboratoriumexperimenten.

Conclusies
Het blijkt gunstig te zijn de aanstootkracht onder een machine te verdelen over een contactvlak met tenminste één dimensie groter dan de golflengte in de scheepsconstructie. In dit rapport worden theoretische en experimentele methoden beschreven waarmee het effect van de verdeelde aanstoting kan worden gekwantificeerd. Twee verschillende meetmethoden, directe admittantiemetingen en constructiegeluidintensiteitmetingen op de ontvangende plaat, leiden tot dezelfde resultaten.

Contents

1 Introduction

The work presented in this report has been performed within the framework of the TNO Defence Research programme in the field of structural acoustics. This programme deals with the development of calculation tools for the prediction of the effect of the design of the seating structure on the vibratory power supplied to ship structures by machinery. One of the aspects that govern the structure-borne noise transmission to the ship structure is the size of the connections between the machine or its seating and the ship structure. Conventionally, noise transmission problems are treated under the assumption of point-like connections between source and receiver, but this assumption is frequently violated in engineering practice. Thus it is important to examine the effects of distributed excitation via large contact areas.

An introductory study of surface excitation on beam- and frame-like systems has been presented in [1]. This study of strip-excited beams and frames clearly demonstrates that effects of distributing the excitation over a large contact area can be both beneficial and detrimental for the reduction of active power transmission at frequencies where the strip length is of the order of magnitude of or larger than the governing wavelength in the receiving structure. Similar results have been found for strip-excitation on an infinitely large homogeneous plate [2]. However, the effect of strip excitation in the vicinity of a structural discontinuity, like a stiffener, on a plate-like structure remains to be investigated. Therefore, this reports describes the results of a combined theoretical and experimental study of strip excitation on an infinitely large homogeneous plate with a single line-stiffener.

2 Theoretical background

This chapter reviews the basic definitions and describes the approach chosen for the theoretical study.

2.1 Surface mobility

It is convenient to handle structural acoustic power transmission by means of mobility theory. The concept of surface mobility is introduced to treat the variation of the stress and velocity distributions over a large contact area. Far a flat contact area S, of arbitrary shape, in the xy-plane, the stress distribution $\sigma(x,y)$ and the corresponding velocity distribution $v(x,y)$ yield the transmitted complex power P :

$$P = \frac{1}{2}\int_S \sigma^*(x,y)\, v(x,y)\, \mathrm{d}x\mathrm{d}y \qquad (1)$$

The total force F is obtained by integration of the stress distribution over the contact area:

$$F = \int_S \sigma(x,y)\,dxdy \tag{2}$$

The velocity distribution is related to the stress distribution via the transfer mobility distributions $\gamma(x,y|x',y')$ of source (subscript 's') and receiver (subscript 'r'):

$$v(x,y) = \int_S \left[\gamma_s(x,y|x',y') + \gamma_r(x,y|x',y')\right]\sigma(x',y')\,dx'dy' \tag{3}$$

In analogy with the definition of point mobility, the surface mobility Y^S may be defined on a power basis:

$$Y^S = \frac{P}{\frac{1}{2}|F|^2} \tag{4}$$

or:

$$Y^S = \frac{\int_S \sigma^*(x,y)\left\{\int_S \left[\gamma_s(x,y|x',y') + \gamma_r(x,y|x',y')\right]\sigma(x',y')\,dx'dy'\right\}dxdy}{\left|\int_S \sigma(x,y)\,dxdy\right|^2} \tag{5}$$

Hence the surface mobility is weighted by the stress distribution and by the mobility distributions of source and receiver in the contact area.

2.2 Strip mobility

As argued in [1] it is worthwhile to study strip excitation, i.e. one dimension of the contact area is smaller than the wavelength while the other can be large, foremost because of an enhanced physical lucidity. The problem can be further simplified by describing the excitation in terms of a stress distribution with a negligibly small source mobility distribution γ_s. Any source can thus be described, by selecting the right stress distribution, taking into account the actual receiver mobility. Then eq.(5), for a strip of length L along the x-axis, simplifies to:

$$Y^{strip} = \frac{\int_{-L/2}^{L/2} \sigma^*(x)\left\{\int_{-L/2}^{L/2} \gamma_r(x|x')\,\sigma(x')\,dx'\right\}dx}{\left|\int_{-L/2}^{L/2} \sigma(x)\,dx\right|^2} \tag{6}$$

2.3 Effective mobility

The effective mobility distribution γ^{eff} is defined as the resulting mobility distribution on the strip, under influence of the complete strip excitation:

$$\gamma^{eff}(x) = \frac{\int_{-L/2}^{L/2} \gamma_r(x|x')\,\sigma(x')\,dx'}{\sigma(x)} \tag{7}$$

Hence, the strip mobility is related to the effective mobility via:

$$Y^{strip} = \frac{\int_{-L/2}^{L/2} \gamma^{eff}(x)\,|\sigma(x)|^2\,dx}{\left|\int_{-L/2}^{L/2} \sigma(x)\,dx\right|^2} \tag{8}$$

2.4 Discretization

For the beam-like receiving structure there exist closed form solutions of the above integral equations (see [1]). This is not the case for plate-like receiving structures and certainly not for a plate with a line stiffener. Therefore the integral equations for the effective mobility, eq.(7), and for the strip mobility, eq.(8), are solved numerically by means of discretization of the stress and mobility distributions. The strip is divided in N sections of equal length $dL=L/N$. In each section n the stress and the mobility are assumed to be distributed uniformly, resulting in discrete forces F_n and transfer mobilities γ_{mn}. Hence the expression for the effective mobility distribution, eq.(7), reduces to:

$$\gamma_n^{eff} = \frac{\sum_{m=1}^{N} \gamma_{nm} F_m}{F_n} \tag{9}$$

where $F_n=\sigma(x_n)dL$. The strip mobility, eq.(8), becomes:

$$Y^{strip} = \frac{\sum_{n=1}^{N} \gamma_n^{eff}\,|F_n|^2}{|F|^2} \tag{10}$$

where $F=\Sigma F_n$, see eq.(2).

The optimum discretization for the transfer mobility distribution is governed by the wavelength in the receiving structure. Six sections per structural wavelength should be

sufficient. Additionally, the discretization depends upon the shape of the stress distribution. Smaller sections may be required if the stress distribution exhibits sharp peaks.

2.5 Transfer mobilities on a line-stiffened plate

The expressions for the transfer mobilities on an infinitely large, homogeneous, thin plate with or without a single line stiffener are derived in [3] and experimentally validated in [4]. The stiffener is modelled by means of a rigid line support along the y-axis, i.e. the plate mobility on the stiffener is zero. The expressions are given in Appendix A.

3 Numerical modelling

3.1 Strip excitation on a homogeneous plate

The effect of strip excitation on an infinitely large homogeneous thin plate in flexure serves as a reference, to be able to separate the effects of distributed excitation from the additional effects due to the introduction of a line stiffener. The problem is studied in the range of Helmholtz-numbers k_bL, based on the flexural wavenumber k_b and strip length L, between 0.1 and 10. Two idealized excitation conditions, a uniform force distribution and a uniform velocity distribution prescribed along the strip, are examined.

Uniform force distribution (soft strip)
The highest Helmholtz-number considered (k_bL=10) corresponds with the shortest wavelength (λ_b=10/2πL). Applying the criterium of six elements per wavelength (see section 2.4) leads to a discretization of the strip into N=10 elements. Figure 1 shows the normalized effective mobility ($\gamma_n^{eff}/NY^{\infty}$) under the strip, for Helmholtz-numbers k_bL=1, 2, 5 and 10. Y^{∞} is the input mobility for point excitation on an infinite plate, x is the coordinate under the strip and x_c is the position of the center of the strip. Because of the uniform force distribution, this mobility corresponds with the velocity distribution under the strip. It is seen that, with increasing Helmholtz-number, the real part of the distribution deviates from the uniform distribution and decreases. The resulting normalized strip mobility (Y^{strip}/Y^{∞}) is shown in Figure 2. Above Helmholtz-number 1 the real part of the strip mobility decreases, which indicates that less power is transmitted via the strip than would be transmitted via point excitation, for the same total force.

Uniform velocity distribution (rigid strip)
The discretization applied for the uniform force distribution does not necessarily apply for the uniform velocity distribution, if the corresponding stress distribution exhibits sharp peaks. The stress distribution that leads to a uniform velocity distribution follows from inversion of the mobility matrix $[\gamma_{nm}]$ for the discretized strip, eq.(9). Figure 3 shows the normalized effective impedance distribution ($\zeta_n^{eff}\, Y^{\infty}$) under the strip, when it is discretized into N=10 elements, for Helmholtz-numbers k_bL=1, 2, 5 and 10. Since the

velocity is uniformly distributed, this normalized impedance distribution is equal to the normalized force distribution. The force appears to be concentrated at the ends of the strip. Hence, the discretization seems to be insufficient. Therefore the procedure has been repeated for N=20 and N=30 elements respectively. The corresponding force distributions are shown in Figure 4 and Figure 5. With increasing number of elements the force maxima shift towards the ends of the strip. Figure 6 shows the resulting normalized strip mobility (Y^{strip}/Y^{∞}) for the uniform velocity distribution, with N=10, 20 and 30, respectively. This strip mobility is calculated on the basis of eq.(4) and the calculated force distribution. The strip mobility for the three different discretizations do not differ significantly. For comparison, the strip mobility for the uniform force distribution (Figure 2) is added in the same figure. Although the force distributions for these two cases are very much different, the strip mobilities show a comparable behaviour. The real part of the strip mobility for the rigid strip is somewhat lower than that for the soft strip, for Helmholtz-numbers between circa 0.3 and 6.

These results for strip excitation on a homogeneous plate agree with those reported in [2].

3.2 Strip excitation on a line-stiffened plate

The effect of introducing a line-stiffener near the position where the plate is excited via a strip is studied. This introduces as an extra parameter the position x_c of the center of the strip, that is oriented along the x-axis, relative to the line-stiffener along the y-axis at x=0. As noted in section 2.5, the line-stiffener is modelled as a rigid line support. This choice excludes the possibility to investigate the effects of excitation by a rigid strip, that imposes a uniform velocity distribution, when the strip crosses the line-stiffener, i.e. $|x_c/L| \leq 1$. The investigation of such effects would require an adaptation of the analytical model for the mobilities on the line-stiffened plate with a description of the finite mobility of the line stiffener.

Figure 7 shows the velocity distribution under the strip for a uniform force distribution, when the strip is centered across the stiffener (x_c/L=0). The velocity at the stiffener equals zero. The curves in Figure 7 do not show this because they are drawn between the calculated results at the center of the 10 elements into which the strip is discretized. At low Helmholtz-numbers the effective mobility is low, since the stiffener blocks the strip motion. At higher Helmholtz-numbers, i.e. shorter wavelengths, where the plate can deform under the strip, the effective mobility increases. The same behaviour is seen in the strip mobility (Figure 8). Figure 9 shows the velocity distribution for a uniform force distribution, when the strip just touches the stiffener (x_c/L=0.5). In this case the strip starts to rotate at low Helmholtz-numbers, which can be most clearly seen for k_bL=2. The real part of the strip mobility (Figure 10) exhibits a maximum at k_bL≈3.5. Figure 11 and Figure 12 show the effective mobility and the strip mobility for a strip that does not touch the stiffener (x_c/L=1.0). In Figure 12 the strip mobilities are compared for a uniform force distribution and a uniform velocity distribution. In the calculation for the uniform velocity distribution the strip is discretized in 30 elements, to capture the stress distribution that is predominantly concentrated at the strip ends, as has been discussed in

section 3.1. The small discontinuity in the curves for the uniform velocity distribution at k_bL≈1.5 is caused by the use of different expressions for the transfer mobilities for low and high Helmholtz-numbers, see Appendix A. Small deviations in the transfer mobilities are amplified in the matrix inversion that is applied to calculate the strip mobility. This effect is of minor importance and does not influence the general conclusions. Figure 13 and Figure 14 show the mobilities for a strip that is somewhat further removed from the stiffener (x_c/L=1.5). It can be seen that the maxima in the real and imaginary parts of the strip mobility shift towards lower Helmholtz-numbers with an increasing distance between the center of the strip and the stiffener.

Figure 15 summarizes the effect of the strip and the line-stiffener on the real part of the strip mobility, i.e. on the power transmission. In this case the strip mobility is shown for Helmholtz-numbers up to 100. The difference between the strip mobilities for a uniform force distribution and a uniform velocity distribution appears to be unimportant. As a general trend, the distributed excitation under a strip results in a decrease with a factor of 2 (3 dB) for each doubling of the Helmholtz-number k_bL, starting at k_bL=2. The presence of the line-stiffener causes a sharp decrease of the strip mobility towards low Helmholtz-numbers. The value of k_bL below which the mobility starts to drop off decreases with increasing distance between the center of the strip and the stiffener. For a uniform force or velocity distribution under the strip, the overall strip mobility is the lowest when the strip is centered across the stiffener.

The results of these numerical simulations agree very well with what has been found for distributed excitation on beam- and frame-like systems [1].

3.3 Area excitation

In addition to the strip mobilities discussed, the same procedure can be applied to calculate the effect of distributed excitation of a two-dimensional area on a plate. Some preliminary calculations have been performed to investigate the effect of extending the width of the strip. A uniform force distribution over a square area of dimensions L×L is considered, both on a homogeneous plate and on a line-stiffened plate (for x_c=0). The area is discretized in 100 equal square elements. Figure 16 shows the resulting real parts of the surface mobility for Helmholtz-numbers k_bL up to 50. The real parts of the corresponding strip mobilities are displayed as a reference in the same figure. It can be seen that the mobilities for the strip and the square area are almost equal at low Helmholtz-numbers, but that at higher Helmholtz-numbers the surface mobilities for the square area excitation decrease much faster with increasing Helmholtz-number than the strip mobilities. One may tentatively conclude that it is advantageous to distribute the total force of a machine over a larger contact area, because this reduces the energy transmission at higher frequencies, although the present calculations only support this for a uniform conphase force distribution. The investigation of the effects of two-dimensional area excitation for different excitation conditions falls without the scope of the present study.

4 Experiments

The results of the numerical simulations of the strip mobility that have been described in sections 3.1 and 3.2 are validated by means of laboratory experiments.

4.1 Experimental arrangement

The experiments have been performed on the same line stiffened perspex plate that has been used in [4], see Figure 17. It is a 20 mm thick perspex plate of 2 x 3 m, hanging vertically, on rubber strings in order to decouple it from vibrations of the building. The line-stiffener is a perspex beam of thickness 10 mm and height 150 mm. The plate is excited by a shaker, via an aluminum strip of 112 mm long, 10 mm wide and 40 mm high. In one of the experiments it has been attempted to create a uniform force distribution under the strip, by applying a thin rubber layer between the strip and the plate, see Figure 18. If the transfer impedance of the rubber layer is much smaller than the input impedances of the strip and the plate, then it converts the uniform velocity of the rigid strip into a uniform force distribution on the plate. The driving force on top of the aluminum strip is measured by a force transducer, the acceleration of the strip by a set of two small accelerometers, the signals of which are added to suppress the rotational motion of the strip. This rotational motion is expected to be negligibly small, because the shaker virtually prevents rotation.

4.2 Characterization of the rubber layer

As argued in section 4.1, the force distribution on the plate is governed by the velocity of the aluminum strip and the transfer impedance of the rubber layer. The latter has been determined experimentally, via the method that is used at TNO-TPD to characterize flexible mountings [5]. The rubber layer is mounted on a cylindrical steel block of mass M=18 kg. The aluminum strip is used as top mass. It is driven by a shaker, like in the arrangement shown in Figure 18. The layer stiffness K and loss factor η are calculated from the measured complex transfer function between the accelerations above (a_t) and below (a_b) the layer:

$$K(1+i\eta) = -M\omega^2 \frac{a_b/a_t}{1-(a_b/a_t)} \qquad (11)$$

The results are shown in Figure 19. The approximate stiffness of the rubber layer is K=9 MN/m. The loss factor appears to be frequency dependent: $\eta=0.007\sqrt{f}$, where f is the frequency in Hz.The deviations from pure stiffness behaviour at frequencies above circa 800 Hz indicate the presence of resonances in the strip.

4.3 Measuring the strip mobility

It is not straightforward to determine the strip mobility Y^{strip} from the experiment. The input mobility Y^{meas} that is measured on top of the aluminum strip has to be corrected for the transmission through the system between the force transducer ad the plate (i.e. the connecting rod, the aluminum strip and, where applicable, the rubber layer). This correction may be performed by modelling the aluminum strip with the connecting rod as a mass (m=0.21 kg, determined by weighing) and the rubber layer as a spring (k=K(1+iη), see section 4.2). The strip mobility is then calculated from:

$$Y^{strip} = \frac{-i\omega/k + (1 - m\omega^2/k)Y^{meas}}{1 - im\omega Y^{meas}} \tag{12}$$

An alternative way to determine the real part of the strip mobility is to measure the power transmitted to the plate and divide this power by the excitation force on the plate, i.e. the measured excitation force corrected for the acceleration of the mass m.

4.4 Power flow measurements

The real part of the strip mobility can be determined by measuring the power that is transmitted to the plate. This has only been done for a strip position that is remote from the stiffener. In that case the power transmission to the plate can be determined from structural intensity measurements on the plate, around the strip. The validity of this method has been checked first, for point excitation in a position at a distance x_s=400 mm from the stiffener, close to the center of the plate in the y-direction. The structural intensity is measured in N=10 positions on a half circle of radius R=200 mm around the excitation position, see Figure 20. At each position n the structural intensity $I_r(n)$ is determined from the imaginary part of the cross-spectrum G_{a1a2} of two accelerometer signals [6]:

$$I_r(n) = \frac{1}{8Y^{\infty}\omega^2}\frac{k_b}{\sin(k_b\Delta)}\,\mathrm{Im}\{G_{a1a2}(n)\} \tag{13}$$

where k_b is the flexural wavenumber, Y^{∞}=0.37·10^{-3} m/Ns the driving point mobility of an infinite plate (20 mm, perspex) and Δ=32.5 mm the separation of the accelerometers. The radius R is slected to maximize the distance between the intensity measurement positions and both the excitation position and the line stiffener (R=x_s/2). The two-channel method is valid for flexural wavelengths smaller than 2R, i.e. for frequencies above circa 500 Hz ($k_b x_s \approx 2\pi$). The separation of the accelerometers is chosen such that it is smaller than one fourth of a flexural wavelength at the highest frequency (5000 Hz). The total power flow is calculated from the measured intensities, assuming that the power flow through the half circle that is not measured is equal to the measured power flow, because of symmetry across the x-axis:

$$P = 2\frac{\pi R}{N}\sum_{n=1}^{N} I_r(n) \tag{14}$$

The input mobility is related to the power flow via eq.(4). The driving force F is measured at the excitation point. Figure 21 shows the real part of the input mobility, normalized with Y^{∞}, for point excitation at a distance of 400 mm from the line-stiffener. The solid line gives the directly measured mobility, using a force transducer and a set of two accelerometers on the indenter at the excitation position, the dashed line is derived from the intensity measurements. The results of boths measurements agree very well. The input mobility at this relatively large distance from the stiffener is almost equal to the infinite plate driving point mobility Y^{∞}. The measured cuves deviates from a straight line at $Y/Y^{\infty}=1$ because of the modal behaviour of the non-infinite experimenal plate. This comparison shows that both methods can be used to determine the power transmission to the plate.

4.5 Strip mobility measurements

The strip mobility has been measured at position x_c=400 mm (L=112 mm, i.e. x_c/L=3.6), for two different stress distributions: a 'rigid' strip, i.e. the aluminum block mounted directly on the plate, and a 'soft' strip, with a rubber layer inserted between the aluminum block and the plate. The input mobility is measured on top of the block and corrected for the mass and stiffness of the block and the rubber layer, to obtain the strip mobility. The real part of the strip mobility is also determined from intensity measurements. Figure 22 shows the results of both mehods for the 'rigid' strip, Figure 23 for the 'soft' strip. Again (see section 4.4) the agreement between the results of both measurement methods is excellent. The general trend of the results is seen to follow the simple model that has been found from the numerical modelling (see chapter 3), for strip excitation remote from stiffeners:

$$\begin{aligned} \mathrm{Re}\{Y^{strip}\} &\approx Y^{\infty} \qquad \text{for} \quad k_b L < 2 \\ \mathrm{Re}\{Y^{strip}\} &\approx \frac{2Y^{\infty}}{k_b L} \qquad \text{for} \quad k_b L \geq 2 \end{aligned} \tag{15}$$

The dotted lines in Figure 22 and Figure 23 give the mobility as measured on top of the aluminum strip. At high Helmholtz-numbers this mobility is lower than the strip mobility due to the acceleration of the mass of the block. Figure 23 shows the damped resonance of the block on the rubber layer at about 1000 Hz (k_bL≈2.4). Figure 24 shows the real and imaginary parts of the strip mobility, derived from the input mobility measurement, together with the results of theoretical predictions, according to the numerical modeling that has been described in chapter 3. The average trend of the measured imaginary parts of the strip mobility starts to deviate from the theoretical predictions above k_bL=3. An explanation for this deviation has not been found. The modal behaviour of the receiving plate largely masks the small differences that might be expected due to the different stress distributions, although one might tentatively conclude that the measured mobilities

confirm the prediction that the mobility for the soft strip ('uniform force') is somewhat higher than that for the rigid strip ('uniform velocity') at Helmholtz-numbers around k_bL=2.

Figure 25 shows the measured mobilities for positions on the stiffener. The driving point mobility on the stiffener is compared with strip mobilities for a rigid strip at x_c/L=0 and x_c/L=0.27. The strip mobilities are almost equal for both positions. They do not show the sharp decrease of the mobility towards low Helmholtz-numbers that is found in the numerical modelling (see Figure 15). The reason for this is clear from the comparison with the measured point mobility on the stiffener. In the numerical model the line stiffener is modelled as a rigid support, hence this point mobility is infinitely small. In the experiment the line stiffener has a finite stiffness, so that the strip mobility at low Helmholtz-numbers is governed by the input mobility of the stiffener. The driving point mobility increases towards k_bL=5 where it appproaches a resonance for longitudinal ('in-plane') waves in the height of the stiffener. This behaviour is not seen in the strip mobilities, because the strip sees the mobility of the stiffener and the strip mobility on the plate in parallel, so that the lowest mobility predominates. At $k_bL \rightarrow 5$ the strip mobility is lower than the point mobility on the beam, as may been seen from comparison with Figure 24. As stated in the beginning of section 3.2, the present model for strip mobility on a line-stiffened plate would require an adaptation to include the effect of the mobility of the stiffener.

5 Conclusions and recommendations

The distribution of the excitation force from a machine on the ship structure over a large contact area is beneficial for the reduction of noise transmission at higher frequencies. The criterium for the ocurrence of this effect is that the contact area should have at least one dimension larger than the governing wavelength in the ship structure.

This general conclusion may be drawn from the results of the theoretical and experimental investigations described in this report. The effect can be quantified in terms of a 'surface mobility', that is defined as the ratio of the total transmitted power via the contact area and the total excitation force in the contact area. Numerical predictions can be made by applying previously derived analytical expressions for driving point and transfer mobilities on plate fields with and without line-stiffener in combination with a discription of the force distribution in the contact area. From numerical simulations it follows that the differences in the power transmission are small for two idealized excitation conditions, a uniform conphase force distribution and a uniform conphase velocity distribution, in spite of large differences in the corresponding spatial force distributions. This conclusion is validated in a series of laboratory experiments.

Two different experimental techniques have been applied to determine the strip mobility for excitation of a line-stiffened plate by a rigid block, that is either mounted directly on the plate, or mounted resiliently via a thin rubber layer. Direct input mobility

measurements on top of the block, corrected for the transmission via the block and its mounting, and structural intensity measurements on the receiving plate yield the same results for the strip mobility.

An important conclusion of this study is the fact that the concept of a 'surface mobility' is valid. This offers the possibility to implement the structure-borne sound transmission via large contact areas in a prediction method in terms of a single mobility. The prediction of the effects of surface excitation across a stiffener on a plate would require an extension of the available model for the rigidly supported plate with a description of the finite mobility of the line-stiffener. Furthermore it is highly relevant to acquire information about the actual force distributions under the mounts of shipboard machinery.

Delft, 23 september 1996 TNO Institute of Applied Physics

dr.ir. C.A.F. de Jong, ir. P.P. Kooyman, ing. F.G.P. van der Knaap

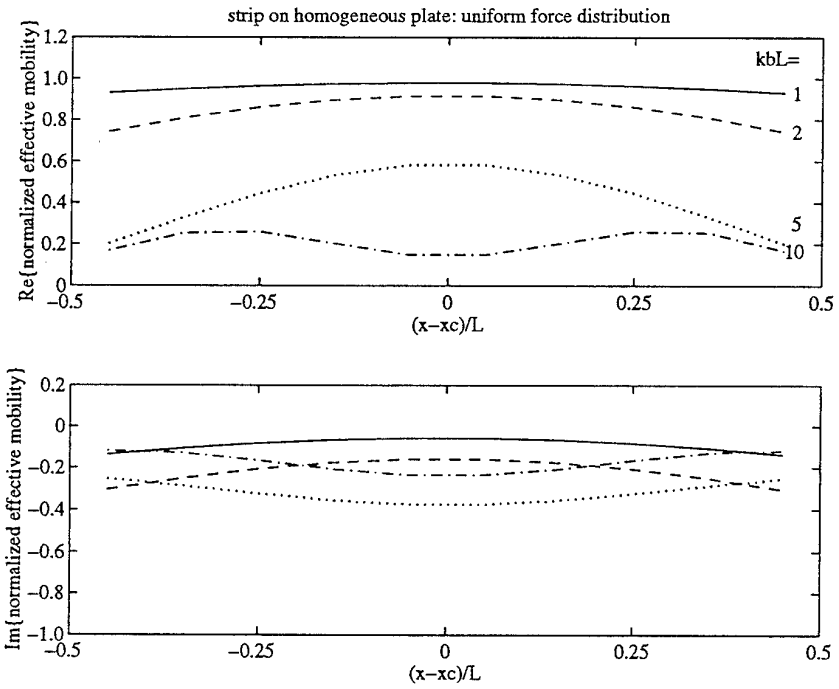

Figure 1: real (top) and imaginary (bottom) part of the normalized effective mobility distribution under a strip with uniform force distribution on an infinite homogeneous plate.

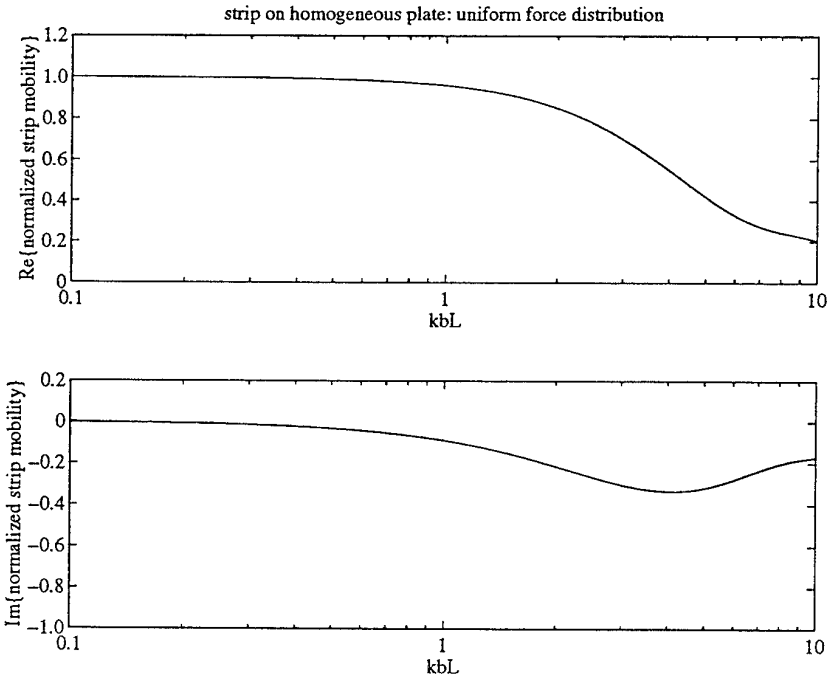

Figure 2: real (top) and imaginary (bottom) part of the normalized strip mobility for a strip with uniform force distribution on an infinite homogeneous plate.

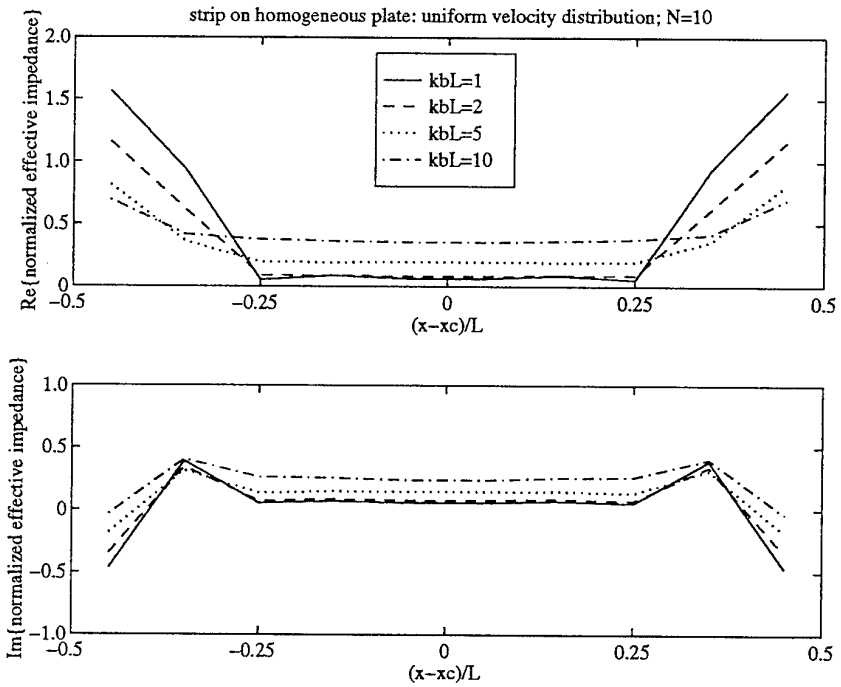

Figure 3: real (top) and imaginary (bottom) part of the normalized effective impedance distribution under a strip with uniform velocity distribution on an infinite plate; N=10.

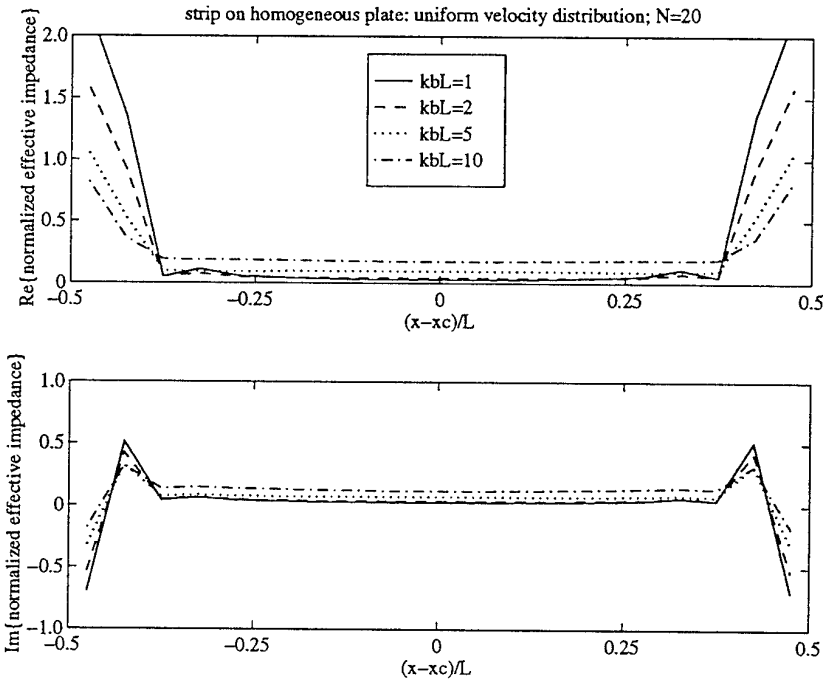

Figure 4: real (top) and imaginary (bottom) part of the normalized effective impedance distribution under a strip with uniform velocity distribution on an infinite plate; N=20.

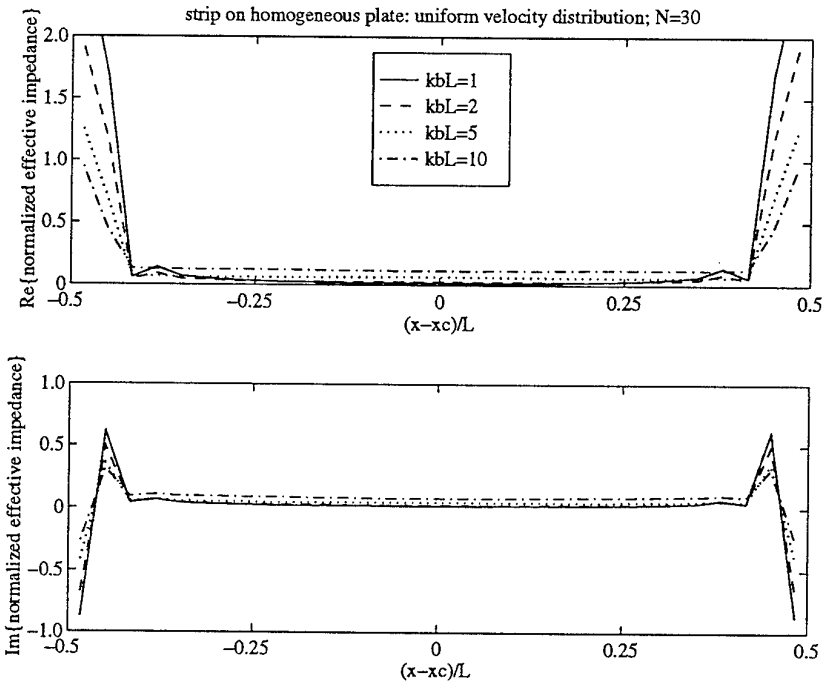

Figure 5: real (top) and imaginary (bottom) part of the normalized effective impedance distribution under a strip with uniform velocity distribution on an infinite plate; N=30.

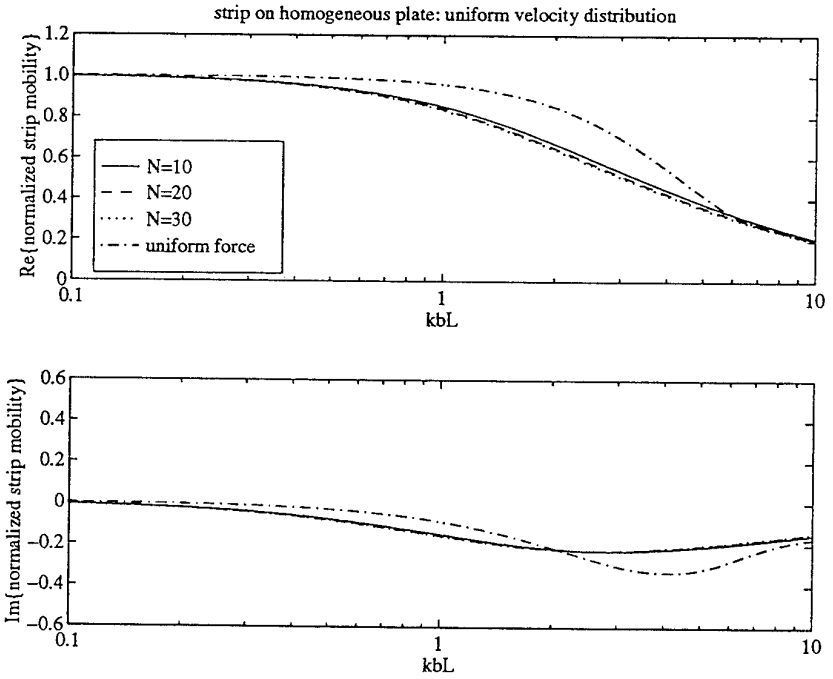

Figure 6: real (top) and imaginary (bottom) part of the normalized strip mobility for a strip with uniform velocity on an infinite plate (N=10, 20 & 30) and for a uniform force distribution.

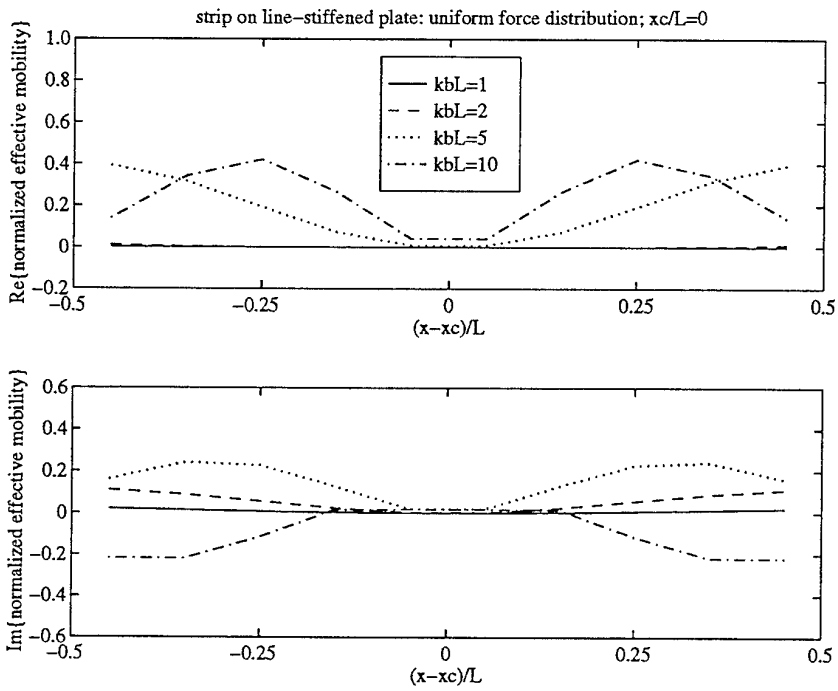

Figure 7: real (top) and imaginary (bottom) part of the normalized effective mobility distribution under a strip with uniform force distribution on a line-stiffened plate; $x_c/L=0$.

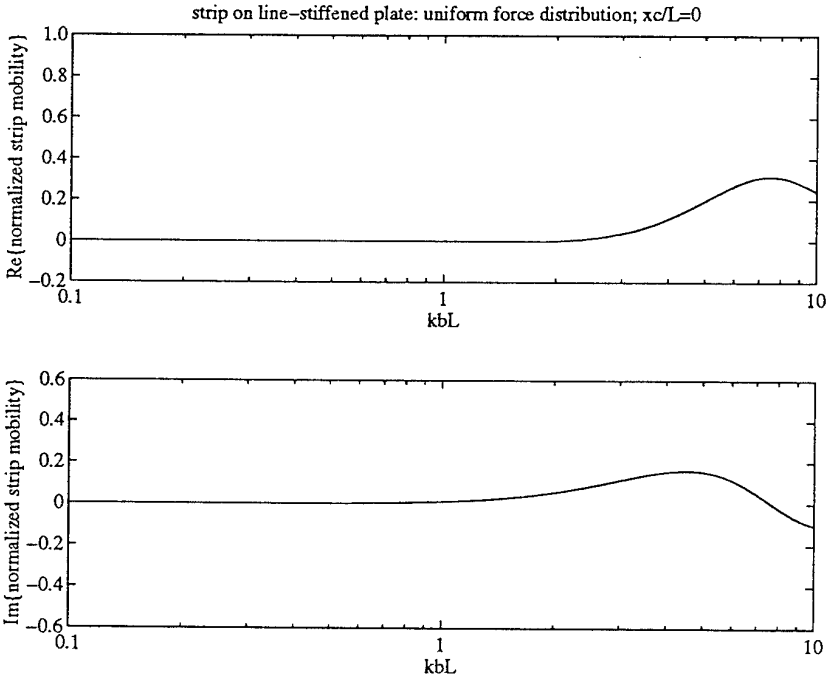

Figure 8: real (top) and imaginary (bottom) part of the normalized strip mobility for a strip with uniform force distribution on a line-stiffened plate; $x_c/L=0$.

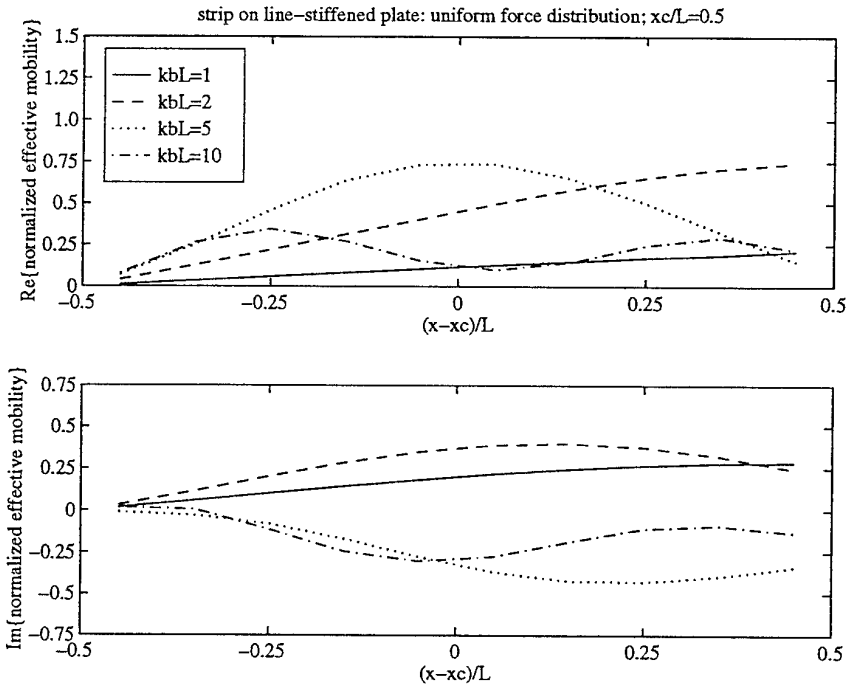

Figure 9: real (top) and imaginary (bottom) part of the normalized effective mobility distribution under a strip with uniform force distribution on a line-stiffened plate; $x_c/L=0.5$.

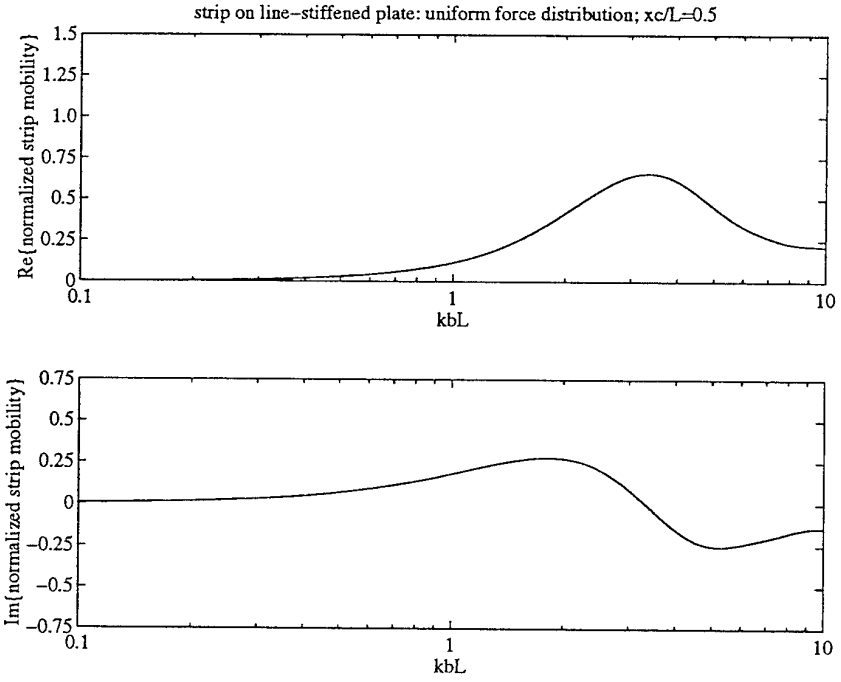

Figure 10: real (top) and imaginary (bottom) part of the normalized strip mobility for a strip with uniform force distribution on a line-stiffened plate; $x_c/L=0.5$.

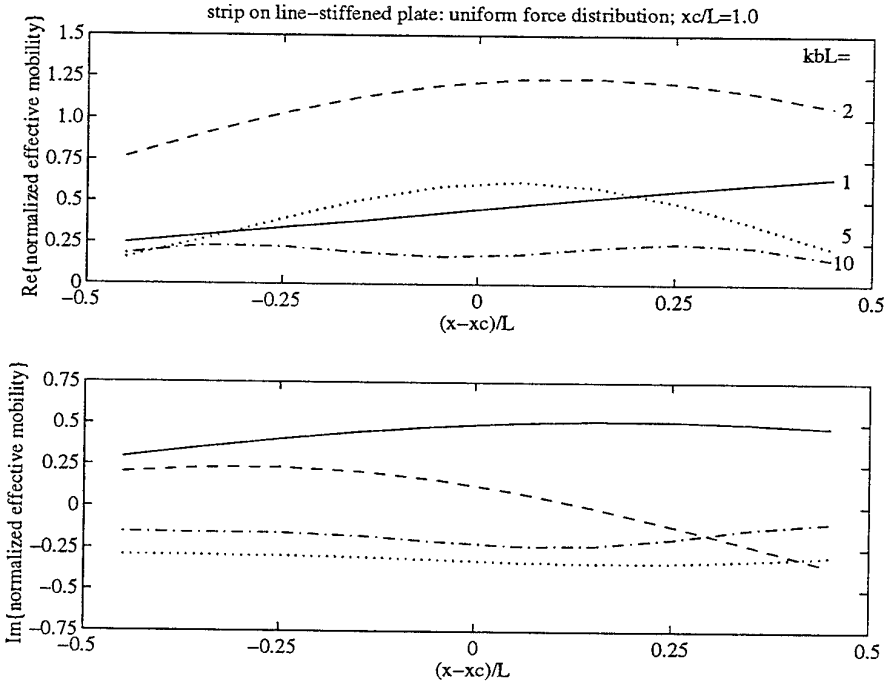

Figure 11: real (top) and imaginary (bottom) part of the normalized effective mobility distribution under a strip with uniform force distribution on a line-stiffened plate; $x_c/L=1.0$.

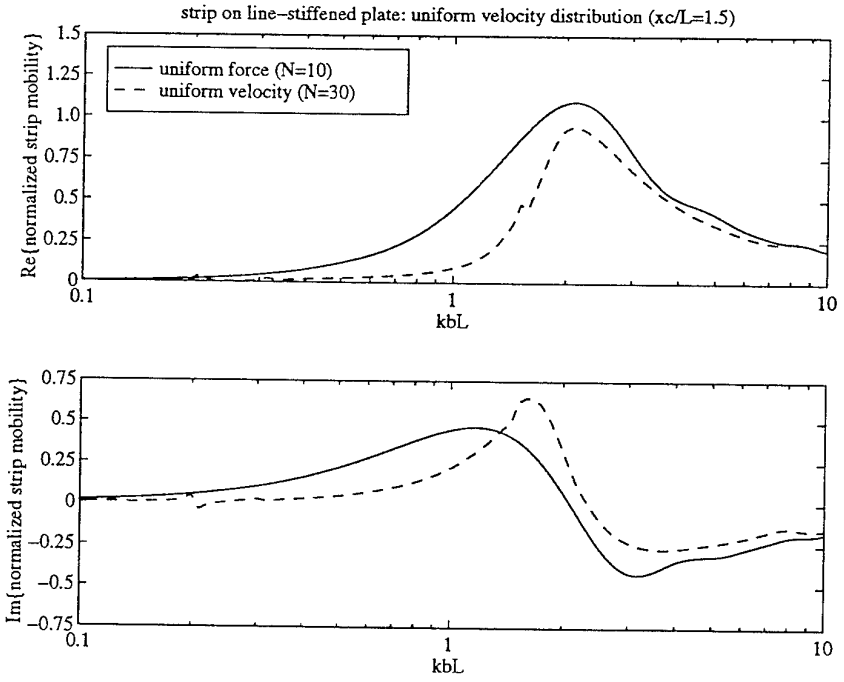

Figure 12: real (top) and imaginary (bottom) part of the normalized strip mobility for a strip with uniform velocity or force distribution on a line-stiffened plate; $x_c/L=1.0$.

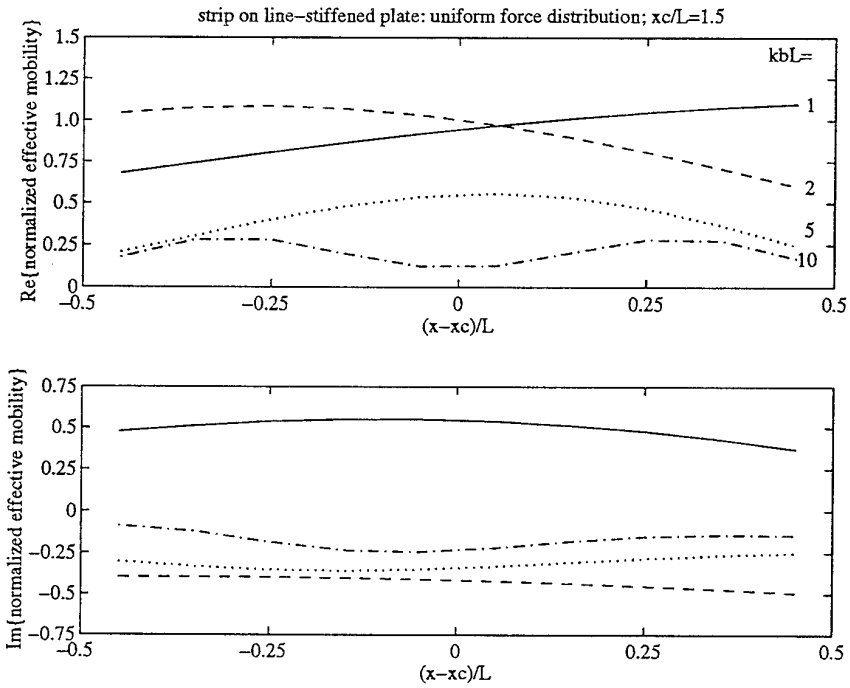

Figure 13: real (top) and imaginary (bottom) part of the normalized effective mobility distribution under a strip with uniform force distribution on a line-stiffened plate; $x_c/L=1.5$.

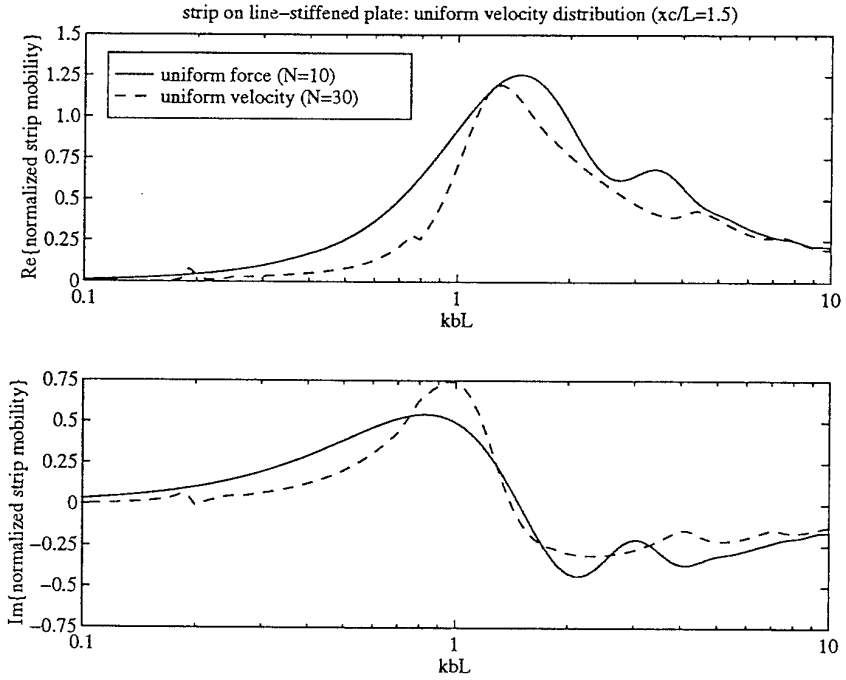

Figure 14: real (top) and imaginary (bottom) part of the normalized strip mobility for a strip with uniform velocity or force distribution on a line-stiffened plate; $x_c/L=1.5$.

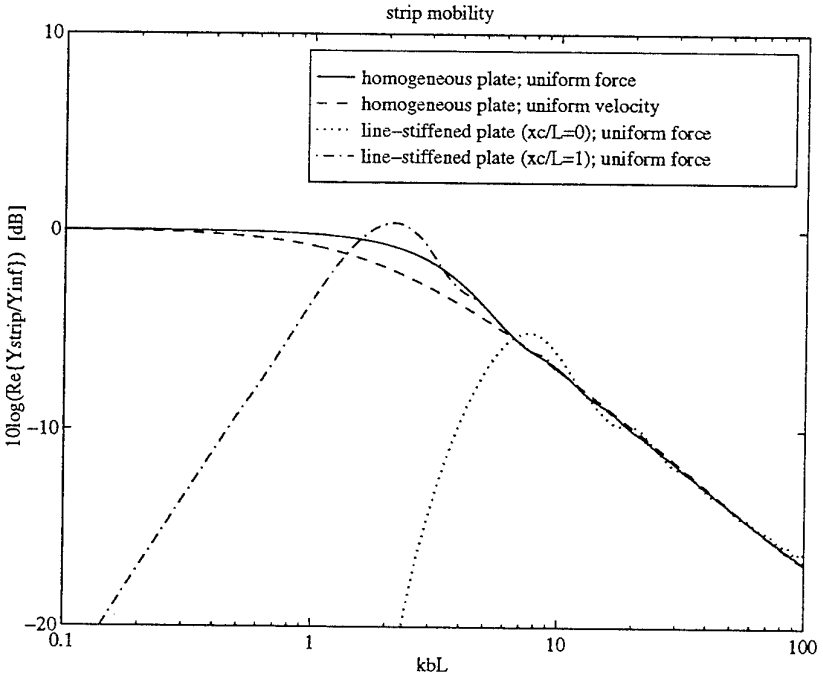

Figure 15: the real part of the normalized strip mobility on a homogeneous and a line-stiffened plate, in dB, compared for different stress distributions under the strip.

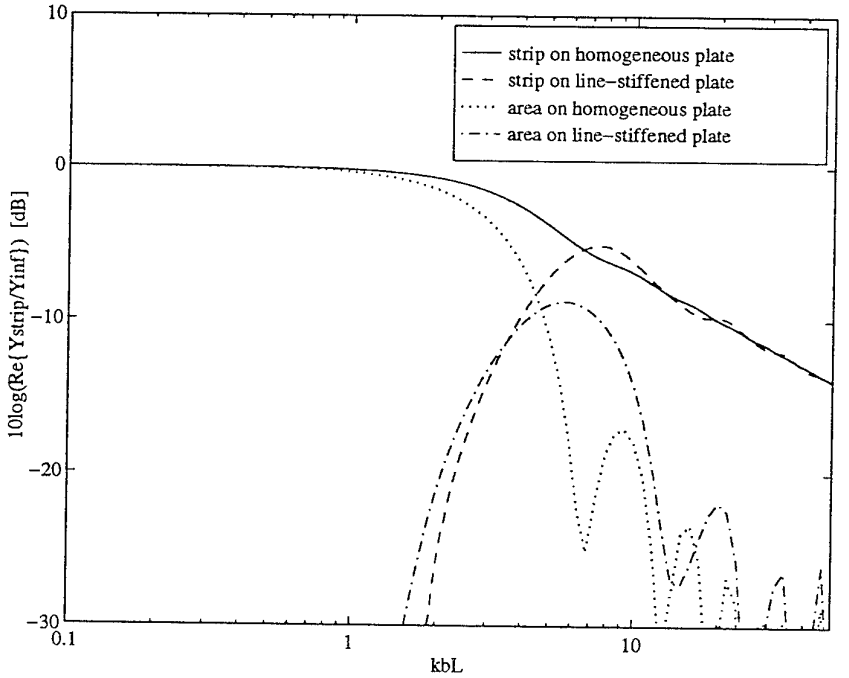

Figure 16: the real part of the normalized mobility for uniform force distribution on a homogeneous and a line-stiffened plate, in dB; for excitation via a strip of length L and via a square area (L×L)

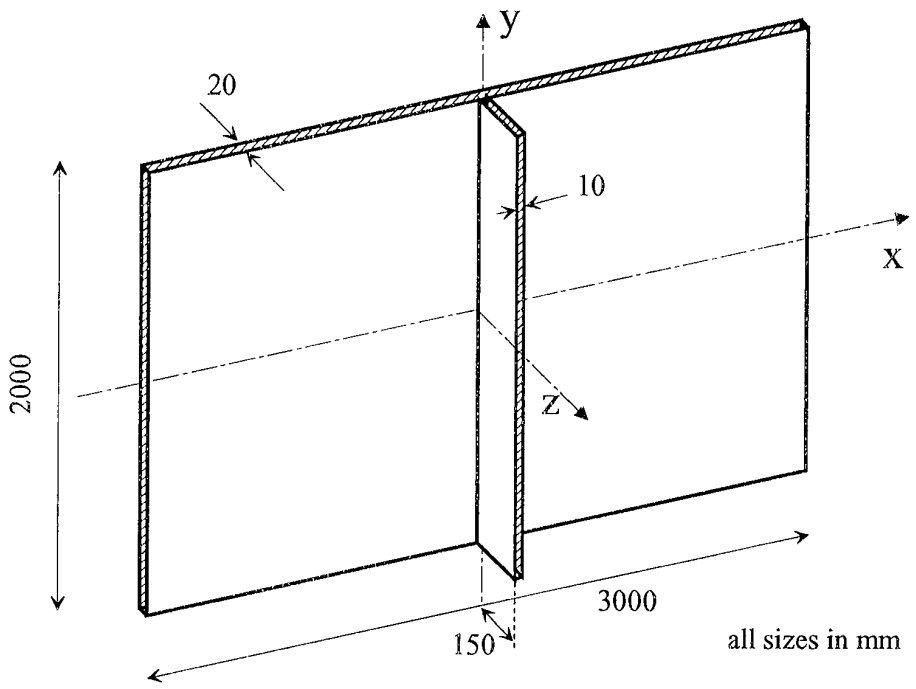

Figure 17: Sketch of the perspex plate on which the experiments have been performed.

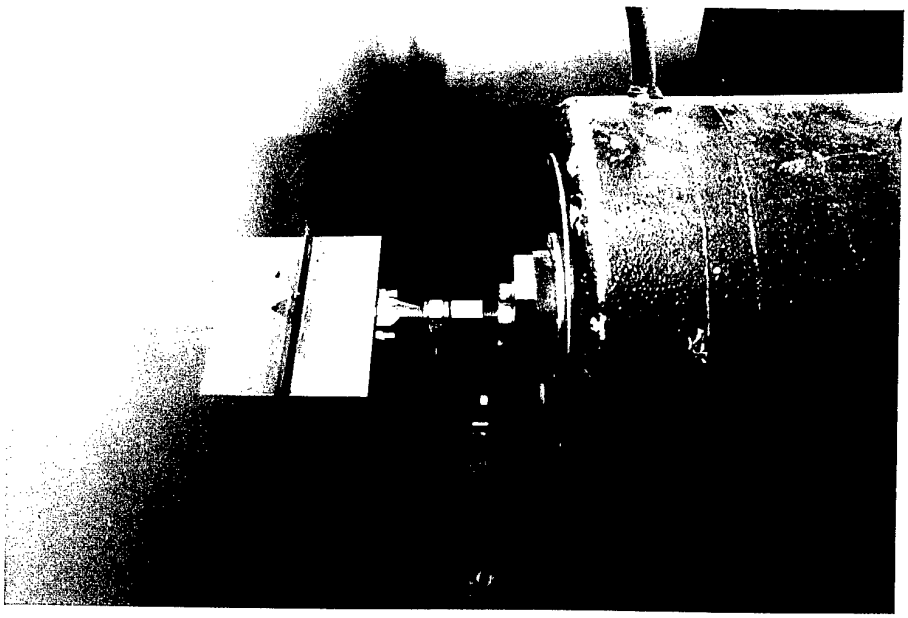

Figure 18: Photograph of the aluminum strip, mounted on the plate via a rubber layer.

The strip is driven by a shaker, via a force transducer. The acceleration of the strip is measured by a set of two small accelerometers.

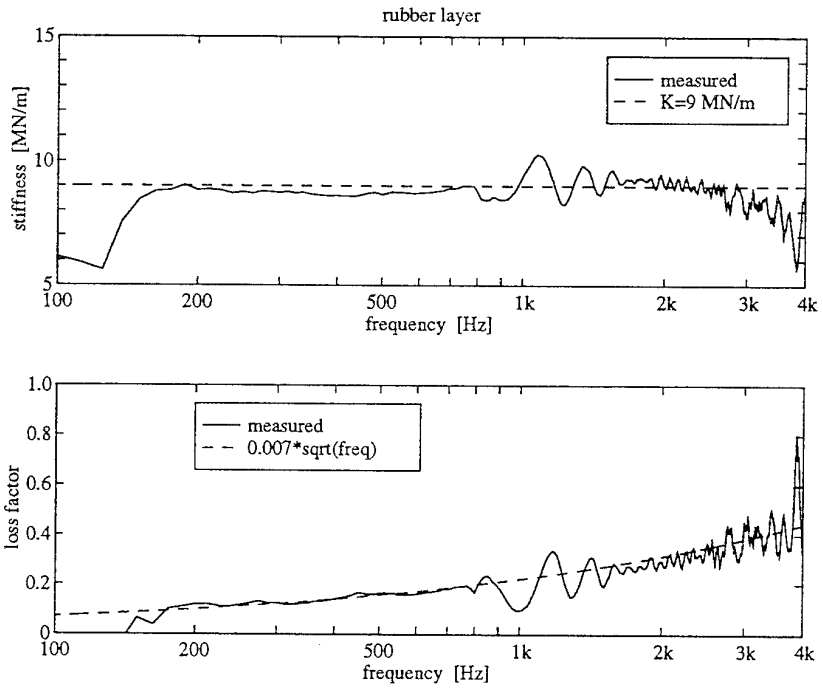

Figure 19: stiffness (top) and loss factor (bottom) of the rubber layer that is applied for the 'uniform force' strip excitation. The dashed curves are fitted to the measured data.

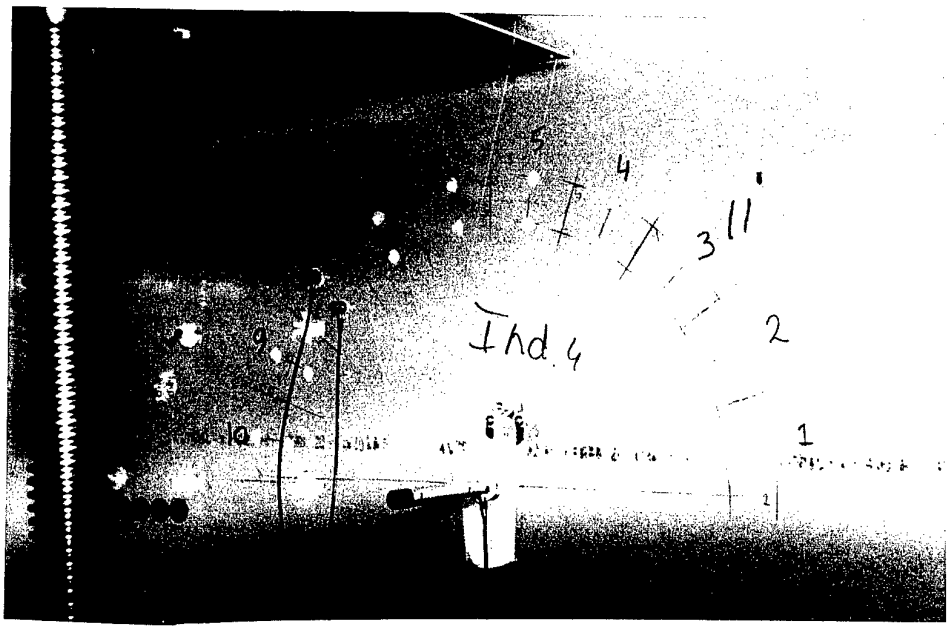

Figure 20: photograph of the power flow measurement for point excitation, using a pendulum. Structural intensity measurements are performed, using two accelerometers, on 10 positions on a half circle.

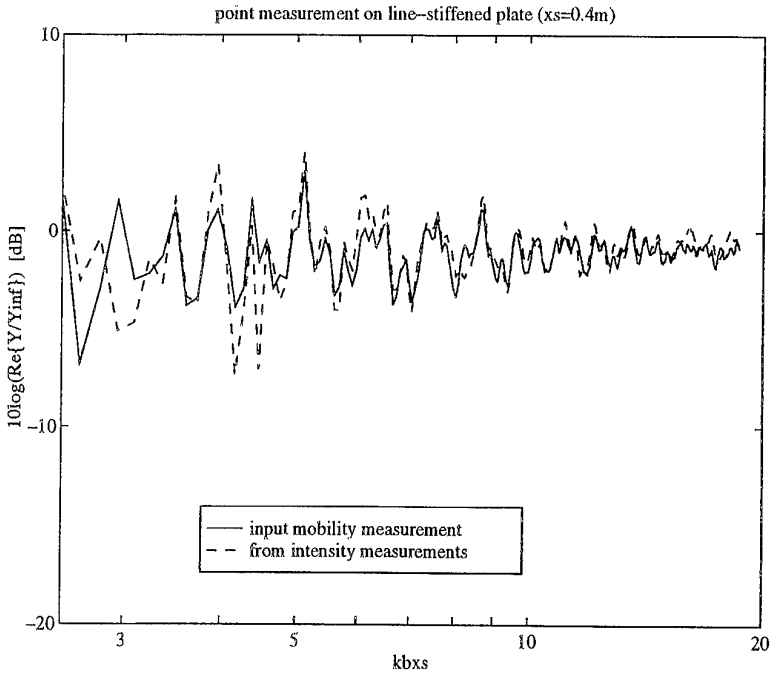

Figure 21: Normalized real part of the input mobility for point excitation at x_s=0.4 m, measured directly and determined from intensity measurements.

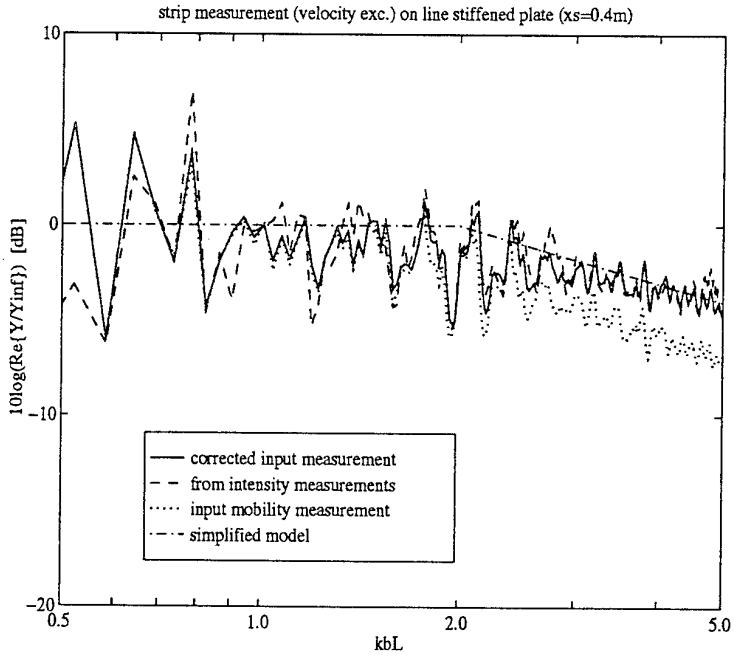

Figure 22: normalized real part of the mobility for a rigid strip (x_c/L=3.6), measured directly, with and without correction for the strip mass, and determined from intensity measurements.

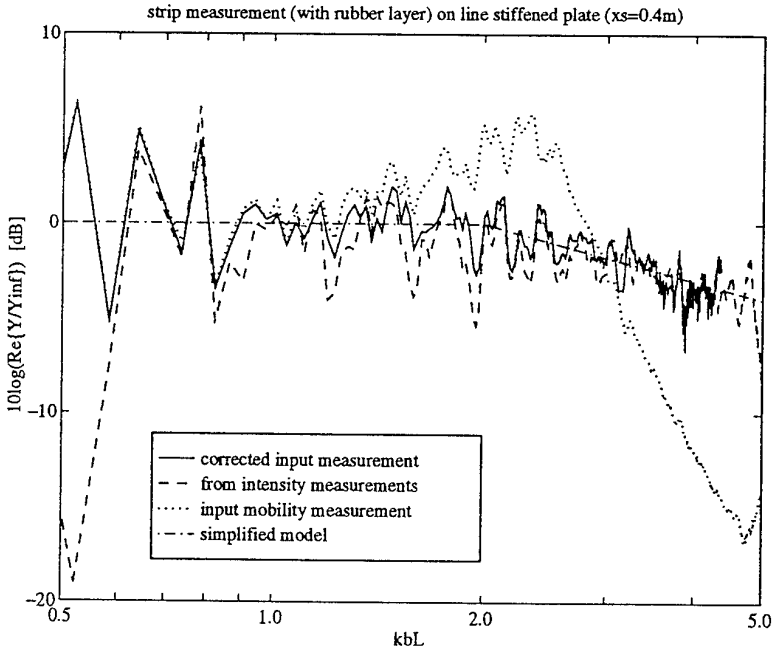

Figure 23: normalized real part of the mobility for a soft strip (x_c/L=3.6), measured directly, with and without correction for the strip mass and stiffness, and determined from intensity measurements.

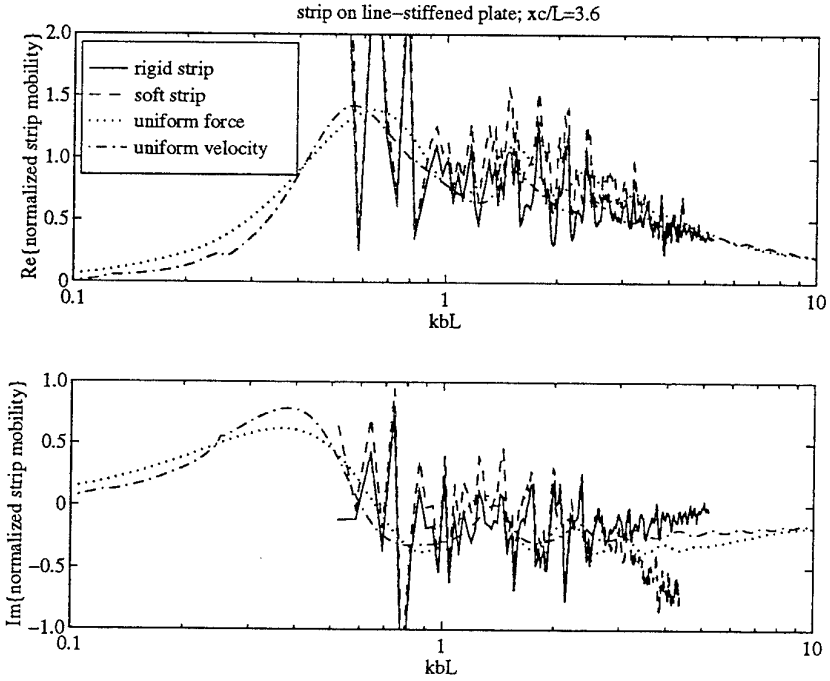

Figure 24: real (top) and imaginary (bottom) part of the normalized strip mobility at x_c/L=3.6. Measurements for rigid and soft strips compared with theoretical predictions.

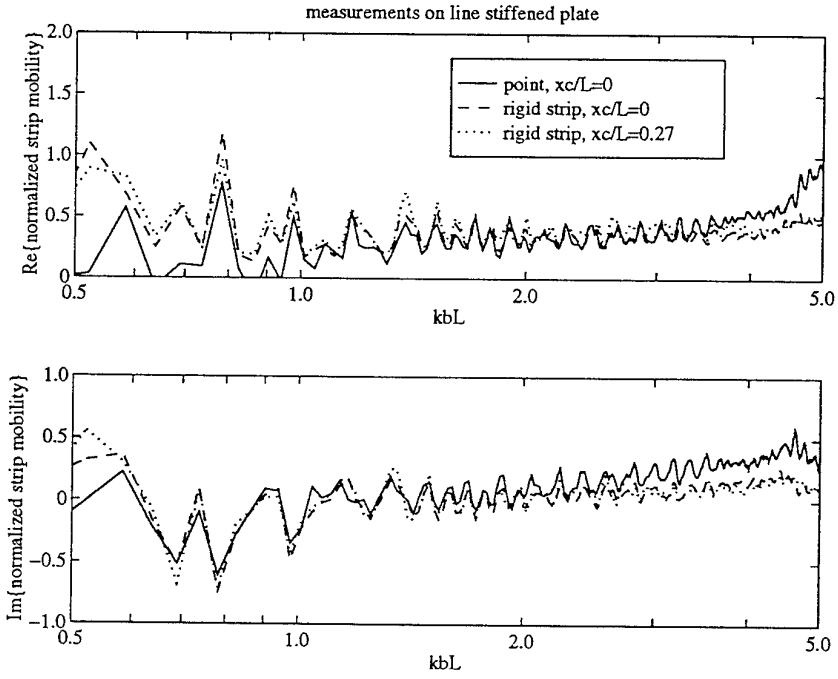

Figure 25: real (top) and imaginary (bottom) part of the normalized mobility for point excitation in x_c/L=0 and excitation via a 'rigid' strip in x_c/L=0 and x_c/L=0.27.

Appendix A: Transfer mobilities on an infinite homogeneous thin plate with a single line discontinuity

This Appendix reviews the expressions for the transfer mobility (see [3],[4] and [7]). The plate lies in the *xy*-plane. The distance between the excitation ("source": *s*) and receiver (*r*) positions is defined as:

$$D_{rs} = \sqrt{(x_r - x_s)^2 + (y_r - y_s)^2} \tag{A.1}$$

and the distance from the receiver position to the perpendicular projection of the source position on the discontinuity as:

$$D_r = \sqrt{x_r^2 + (y_r - y_s)^2} \tag{A.2}$$

The bending wave propagation on an infinite plate is governed by the propagation function:

$$\Pi_0(k_B r) = H_0^{(2)}(k_B r) - H_0^{(2)}(-ik_B r) \tag{A.3}$$

where k_B denotes the bending wavenumber, r the distance and $H_n^{(2)}$ the complex Hankel function of the second kind of order n. The 'first order' propagation function appears when the propagation function is derived with respect to its argument:

$$\Pi_1(k_B r) = -\frac{\mathrm{d}\,\Pi_0(k_B r)}{\mathrm{d}\,k_B r} = H_1^{(2)}(k_B r) + iH_1^{(2)}(-ik_B r) \tag{A.4}$$

For the transfer mobilities on an infinite plate with a single line discontinuity three different approximate expressions are used for different conditions, that are determined by the source and receiver positions, relative to the line discontinuity along the *y*-axis at x=0, and by the Helmholtz-number (explained below) :

- for $|x_r / x_s| \geq 1$ and 'high' Helmholtz numbers:

$$Y_{vzFz}(x_r|x_s) \approx Y^{\infty}\left\{\Pi_0(k_B D_{rs}) - \frac{1+i}{2}\left(e^{-ik_B|x_r|} - ie^{-k_B|x_r|}\right)\Pi_0(k_B D_r)\right\} \tag{A.5}$$

- for $|x_r / x_s| \geq 1$ and 'low' Helmholtz numbers:

$$Y_{vzFz}(x_r|x_s) \approx Y^{\infty}\frac{k_B x_s x_r}{D_r}\Pi_1(k_B D_r) \tag{A.6}$$

- for $|x_r / x_s| < 1$ (reciprocal expression) :

$$Y_{vzFz}(\boldsymbol{x}_r|\boldsymbol{x}_s) = Y_{vzFz}(\boldsymbol{x}_s|\boldsymbol{x}_r) \tag{A.7}$$

The first part of eq.(A.5), i.e. $Y^{\infty}\Pi_0(k_B D_{rs})$, gives the transfer mobility on a homogeneous plate, without line stiffener. The second part of this equation expresses the effect of reflection at the line-stiffener.

It appears to be necessary to apply the 'low' Helmholtz number expression, because the 'high' Helmholtz number expression underestimates the transfer mobilities for positions on the same side of the discontinuity and overestimates the transfer mobilities across the discontinuity. This leads to erroneous results in the integration that is performed to calculate the effective and the strip mobilities. The transition point between 'low' and 'high' Helmholtz numbers is chosen where the spectra of the two approximations cross or where they start to diverge. The Helmholtz number at which this occurs is different for the real and the imaginary part of the transfer mobilities. The transition point has been determined visually from a series of plots of transfer mobilities for different source and receiver positions, see figures A1, A2, A3 and A4. An appropriate choice for the transition point appears to depend upon the Helmholtz number based on the distance from the receiver position to the perpendicular projection of the source position on the discontinuity D_r :

$$\begin{aligned} &\text{transition point at } \; k_B D_r = 0.8 \quad \text{for } \mathrm{Re}\{Y_{vzFz}\} \\ &\text{transition point at } \; k_B D_r = 0.1 \quad \text{for } \mathrm{Im}\{Y_{vzFz}\} \end{aligned} \tag{A.8}$$

Note that reciprocal expression is taken if the receiver position is closer to the discontinuity than the source position. In that case the transition point is based on the D_r after interchanging the source and receiver positions.

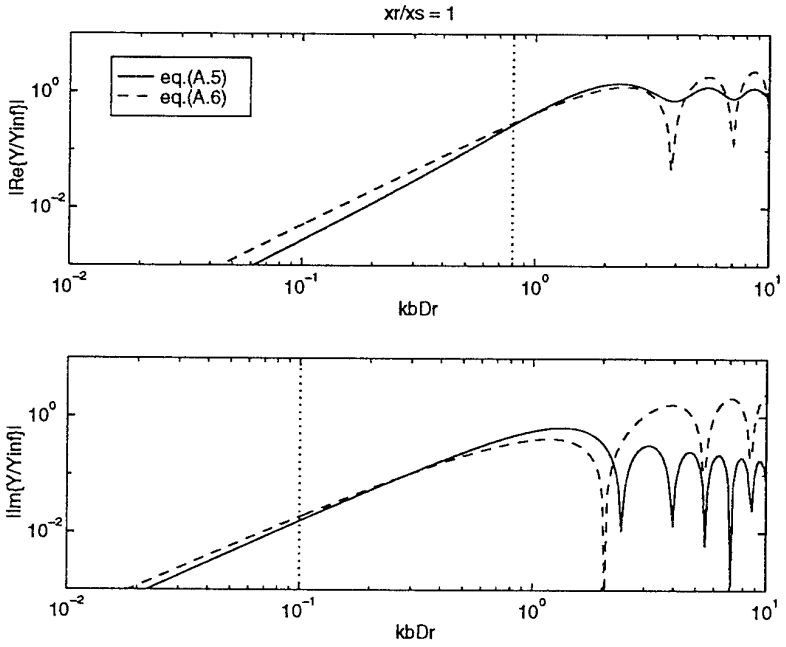

Figure A1: Transfer mobility for x_r/x_s=1, according to eq.(A.5) and eq.(A.6). The dottted line indicates the chosen transition point.

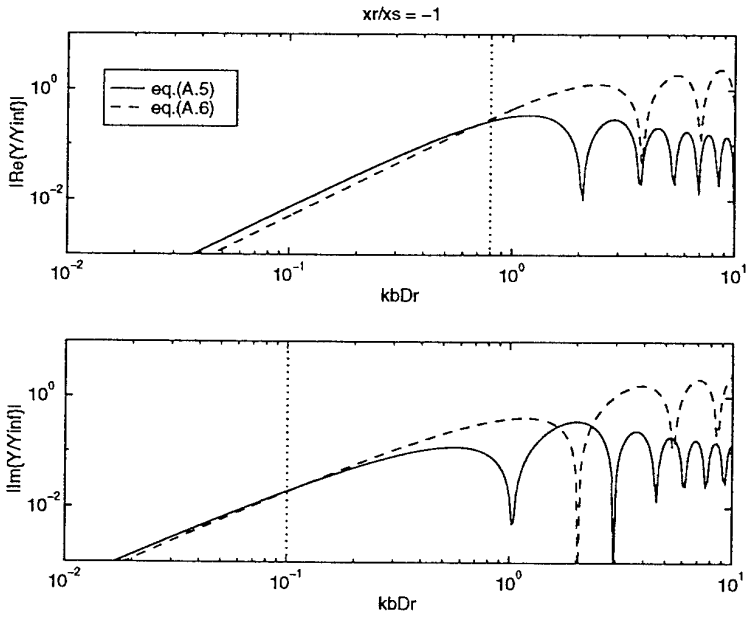

Figure A2: Transfer mobility for x_r/x_s=-1, according to eq.(A.5) and eq.(A.6). The dottted line indicates the chosen transition point.

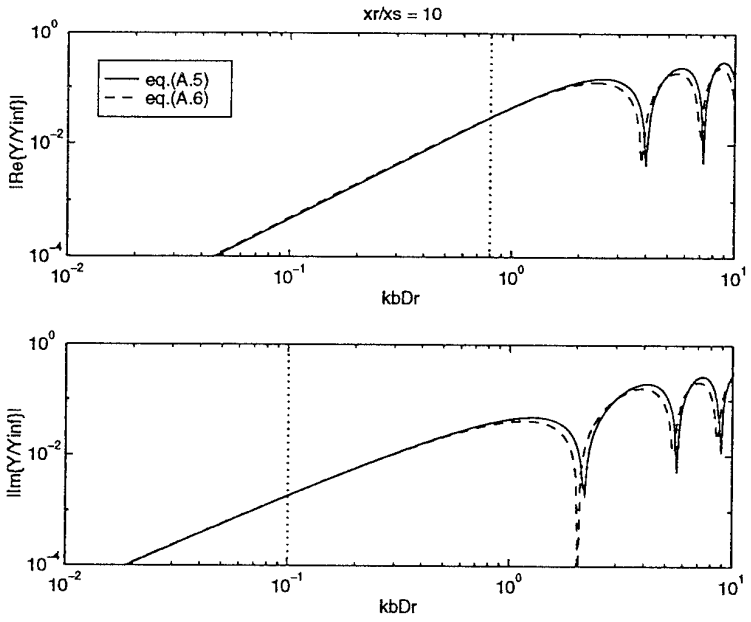

Figure A3: Transfer mobility for x_r/x_s=10, according to eq.(A.5) and eq.(A.6). The dottted line indicates the chosen transition point.

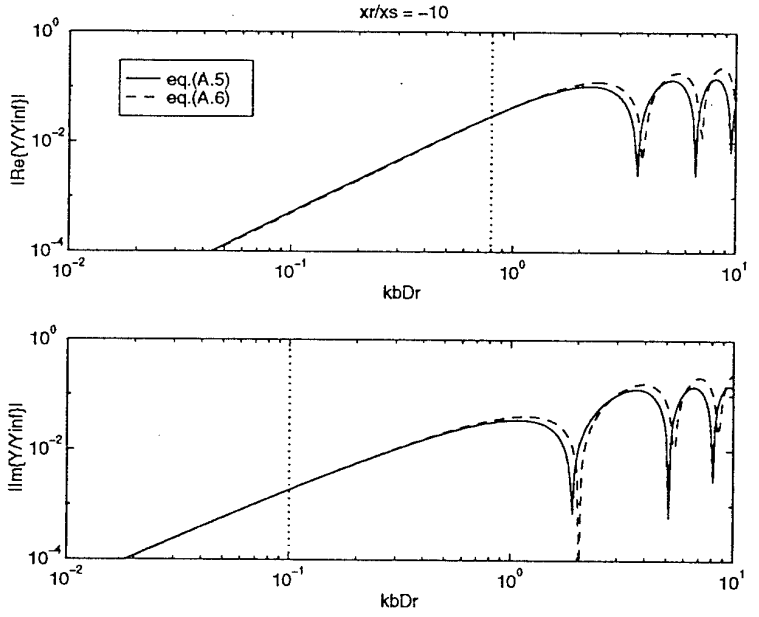

Figure A4: Transfer mobility for x_r/x_s=-10, according to eq.(A.5) and eq.(A.6). The dottted line indicates the chosen transition point.

References

1. B.A.T. Petersson: Surface excitation; part I: Theoretical background and introductory study of beam- and frame-like systems. TPD-HAG-RPT-930216, 1993

2. P. Hammer & B.A.T. Petersson: Strip excitation, part I: strip mobility. *Journal of Sound and Vibration* **129**(1), 119-132, 1989

3. B.A.T. Petersson: Preliminaries for pure transfer mobilities: Force excited plate-like structures. TPD-HAG-RPT-940187, 1994

4. E.J.M. Nijman, F.G.P. van der Knaap & C.A.F. de Jong: Pure transfer mobilities of plate-like structures: experiments. TPD-HAG-RPT-940229, 1995

5. J.W. Verheij: Multi-path sound transfer from resiliently mounted shipboard machinery. PhD Thesis, TNO Institute of Applied Physics, Delft, 1982

6. J.W. Verheij: Cross spectral density methods for measuring structure-borne power flow on beams and pipes. *Journal of Sound and Vibration* **70**(1), 133-138, 1980

7. F.G.P. van der Knaap & C.A.F. de Jong: Transfer and cross transfer mobilities on plate-like structures: experiments. TPD-HAG-RPT-960092, 1996 (Appendix B)

REPORT DOCUMENTATION PAGE (MOD-NL)

1. Defense report number (MOD-NL)	2. Recipient's accession number	3. Performing organization report number
RP-96-0210		TPD-HAG-RPT-960132
4. Project/Task/Work unit no.	5. Contract number	6. Report date
627.190	A94/KM/155	23 September 1996
7. Number of pages (excl. RDP)	8. Number of references	9. Type of report and dates covered
32	7	part report

10. Title and subtitle

Surface excitation: A theoretical and experimental study of strip mobility on a line-stiffened plate.

11. Author(s)

dr.ir. C.A.F. de Jong, ir. P.P. Kooyman & ing. F.G.P. van der Knaap

12. Performing organization name(s) and address(es)

TNO Technisch Physische Dienst, Stieltjesweg 1, 2628 CK Delft

13. Sponsoring/monitoring agency name(s) and address(es)

TNO-Defense Research, Schoemakerstraat 97, 2628 CK DELFT
Ministry of Defence (Navy), Van der Burchlaan 31, 2597 PC 's-GRAVENHAGE

14. Supplementary notes

"ongerubriceerd" is equivalent to Unclassified

15. Abstract (maximum 200 words, 1044 byte)

Theoretical and experimental methods are described, that can be used to quantify the effects of surface excitation on line-stiffened plate structures. These methods are of relevance for the study of structure-borne noise transmission from shipboard machinery to underwater. It is shown that the distribution of the excitation force from a machine on the ship structure over a large contact area is beneficial for the reduction of noise transmission at higher frequencies. The criterium for the ocurrence of this effect is that the contact area should have at least one dimension larger than the governing wavelength in the ship structure. The results of laboratory experiments support this conslusion. Two different experimental techniques, direct mobility measurements and structural intensity measurements on the receiving plate, lead to the same results.

16. Descriptors

Vibration of elastic bodies, wave propagation
Underwater external noise
Mechanical impedance

identifiers

323F R14GF
R08L 328EA
332A W12C

17a. Security classification (of report)	17b. Security classification (of page)	17c. Security classification (of abstract)
ongerubriceerd	ongerubriceerd	ongerubriceerd

18. Distribution/Availability statement	17d. Security classification (of titles)
Distribution according to agreed list. Additional availability via TNO-TPD (subject to TNO-DO and/or MOD/Navy approval).	ongerubriceerd

Distributielijst

1.	DWOO	*
2.	HWO-CO	**
3.	HWO-KM	**
4.	HWO-KL	**
5.	HWO-KLu	**
6.	Ministerie van Defensie, Dir. Materieel KM, afdeling Scheepsbouw, ing. H. Hasenpflug.	
7.	Ministerie van Defensie, Dir. Materieel KM, afdeling Scheepsbouw, P. van der Gaag.	
8.	Ministerie van Defensie, Dir. Materieel KM, afdeling Scheepsbouw, ir. P.J. Keunig.	
9.	TNO-TPD-TU Delft, Hoofdafdeling Geluid, Afdelingsleider Geluidarm Construeren, ir. J.C. Vellekoop*.	
10.	TNO-TPD-TU Delft, Hoofdafdeling Geluid, Afdeling Geluidarm Construeren, dr.ir. C.A.F. de Jong*.	
11.	TNO-TPD-TU Delft, Hoofdafdeling Geluid, Afdeling Geluidarm Construeren, dr. B.A.T Petersson*.	
12.	TNO-TPD-TU Delft, Hoofdafdeling Geluid, Afdeling Geluidarm Construeren, ing. F.G.P. van der Knaap*.	
13.	TNO-TPD-TU Delft, Hoofdafdeling Geluid, Afdeling Geluidarm Construeren, prof.dr.ir. J.W. Verheij*.	
14.	TNO-TPD-TU Delft, Hoofdafdeling Geluid, Afdeling Geluidarm Construeren, ing. W.C. Verboom*.	
15.	TNO-TPD-TU Delft, Hoofdafdeling Geluid, Afdeling Geluidarm Construeren, ir. P.P. Kooijman*.	
16.	TNO-DO*.	
17.	TNO-TPD-TU Delft, Hoofdafdeling Geluid, Archief*.	
18. (t/m 20.)	Bibliotheek KMA***	

Indien binnen de krijgsmacht extra exemplaren van dit rapport worden gewenst door personen of instanties die niet op de verzendlijst voorkomen, dan dienen deze aangevraagd te worden bij het betreffende Hoofd Wetenschappelijk Onderzoek of indien het een K-opdracht betreft, bij de Directeur Wetenschappelijk Onderzoek en Ontwikkeling.

* Alijd een volledig rapport.

** Indien opdrachtgever een volledig rapport, anders een beperkt rapport.

*** 3 volledige rapporten indien het rapport ongerubriceerd of ongemerkt is, anders 1 volledig rapport.